Conformational Flexibility of α-Lactalbumin Related to its Membrane Binding Capacity

ARTICLE *in* JOURNAL OF MOLECULAR BIOLOGY · JULY 2005

Impact Factor: 4.33 · DOI: 10.1016/j.jmb.2005.04.020 · Source: PubMed

4 AUTHORS, INCLUDING:

Oyvind Halskau
University of Bergen
32 PUBLICATIONS **575** CITATIONS
SEE PROFILE

Jarl Underhaug
University of Bergen
21 PUBLICATIONS **283** CITATIONS
SEE PROFILE

Aurora Martínez
University of Bergen
150 PUBLICATIONS **3,682** CITATIONS
SEE PROFILE

doi:10.1016/j.jmb.2005.04.020 J. Mol. Biol. (2005) 349, 1072–1086

JMB

Available online at www.sciencedirect.com

SCIENCE DIRECT®

ELSEVIER

Conformational Flexibility of α-Lactalbumin Related to its Membrane Binding Capacity

Øyvind Halskau[1], Jarl Underhaug[2], Nils Åge Frøystein[2] and Aurora Martínez[1]*

[1]*Department of Biomedicine University of Bergen, Jonas Lies vei 91, 5009-Bergen, Norway*

[2]*Department of Chemistry University of Bergen, Allégaten 41, N-5007 Bergen, Norway*

**Corresponding author*

Different folding states of the small, globular milk protein bovine α-lactalbumin (BLA) induced by the anionic surfactant sodium dodecylsulphate (SDS) have been examined by fluorescence spectroscopy, CD and NMR. The solution structure of the protein in the absence of SDS was also determined, indicating fluidity even under native conditions. BLA is partly denatured to a molten globule (MG)-like state by micromolar concentrations of SDS, and the transitions from native to MG-like state are dependent on pH, the protein being more sensitive to the surfactant at pH 6.5. As indicated by measurements of the intrinsic emission fluorescence, the tertiary structure disappears at lower concentrations of SDS than most of the secondary structure, as estimated from CD data. The MG-like state induced by low concentrations of SDS is not observable by NMR, and is probably fluctuating and/or aggregating. At higher concentrations of SDS above the critic concentration of micelles, an NMR-observable state reappears. This micelle-associated conformer was partially assigned, and found to bear strong resemblance to the acid-trifluoroethanol state, retaining weakened versions of the A and C helix of native BLA. We discuss the results in terms of the inherent flexibility of the protein, and its ability to form multiple folding states and to bind to membranes. Also, we propose that proteins with stable MG-like conformers can have these states stabilized by low levels of compounds with surfactant properties *in vivo*.

Keywords: surfactants; molten globule; flexibility; membrane binding; α-lactalbumin

Introduction

Partly denatured, fluid protein folding states, usually called molten globule (MG) states, have received a steadily increasing amount of attention over the past two decades. Much evidence for the existence of such states has been accumulated, as has knowledge of their stability, dynamics and spectroscopic characteristics.[1–4] While the ability of certain proteins to form MG states is firmly established, there is still no clear picture of how and when the MG state appears in living systems. In this regard, several different phenomena have been noticed and received attention. First, conditions necessary to stabilize many MG states are found at the interface of negatively charged membranes;[5–8] secondly, MG states are thought to be central to protein folding, and misfolding is frequently reported as important in diseases such as Parkinson's, Alzheimer's, scrapie and bovine spongiform encephalopathy;[9,10] thirdly, there are many proteins, or protein domains, that are best understood as being intrinsically disordered, a property that conflicts with the standard structure–function paradigm.[11–21]

α-Lactalbumin (α-LA), a small milk-protein whose MG states have been prepared by a variety of methods, has been under intensive scrutiny. The formation of the MG state under various conditions, low pH, removal or addition of metal ions at elevated temperatures, binding to membranes,

Abbreviations used: α-LA, α-lactalbumin; BLA, bovine α-lactalbumin; CMC, critic micelle concentration; MG, molten globule; TFE, trifluoroethanol; NOE, nuclear Overhauser effect; NOESY, NOE spectroscopy; CSI, chemical shift indexing; TOCSY, total correlated spectroscopy.

E-mail address of the corresponding author: aurora.martinez@biomed.uib.no

reduction of disulphide bonds and solvation in alcohols, has been investigated in numerous studies.[2,22–26] The intrinsic emission fluorescence spectra of these states are characterized by higher emission intensity than for the native protein and wavelength maxima (λ_{max}) around 338–343 nm,[2,23,24,26,27] while complete denaturation of α-LA by urea results in an emission λ_{max} at 353 nm.[28] The numerous MG-states reported for this protein offer the possibility to discern differences among these non-native, fluctuating states and possibly link them to physiological effects. For instance, Alexandrescu *et al.* have shown by NMR and other spectroscopic techniques that it is possible to discern the acid-induced MG state from another MG-like state prepared at low pH in trifluoroethanol (TFE).[24] Furthermore, there is evidence from spectroscopic and hydrogen exchange experiments that membranes of different lipid compositions stabilize distinct, non-native MG-like conformers of α-LA.[29,30] Such differentiation may be found for MGs of other proteins. Reports show that it is possible to modulate the characteristics of the acid MG state cytochrome *c* by the ionic size and concentration of the anions.[31]

The denaturing properties of molar concentrations of the anionic surfactant sodium dodecylsulphate (SDS) are well known and there have been a few reports on proteins having their secondary and tertiary structure modified by millimolar quantities of surfactants.[32–34] Hamada & Takeda reported a system studied at pH 7.0 and examined by circular dichroism (CD), where α-LA interacts with SDS. Loss of tertiary structure was reported to be followed by an increase in helicity, and a decrease in β-sheet content.[34] Also, Chattopadhyay *et al.* reported the refolding of cytochrome *c* to distinct MG-like states under strongly denaturing conditions in the presence of similar surfactants.[33]

Here, we present a study that explores the conformational flexibility of bovine α-LA (BLA) by use of NMR, CD and fluorescence spectroscopy. Three different situations are explored: the native BLA structure, which by NMR appears quite fluid; the protein in the presence of micromolar concentrations of SDS, which yields pH-dependent MG-like states; and the protein bound to SDS micelles. The latter state corresponds closely to the state induced by TFE and low pH,[24] conditions mimicking the chemical environment near negatively charged membranes.[5] This SDS-bound state thus appears to have relevance for understanding the conformation of the protein bound to negatively charged membranes. There are numerous studies using micelles of different surfactants as membrane mimics, ranging from CD, infrared (IR) and fluorescence studies of peptides embedded in lipid micelles, to full structural characterization of micelle-embedded proteins by NMR.[35–37] Micellar environments are well known for inducing secondary structural changes.[38,39] The former work compares a fusogenic peptide structure in detergent micelles to its structure in 30% TFE, finding some differences. Thus, we discuss the micelle-bound state of BLA in light of previous studies on the conformation of the protein in TFE,[40,41] and of our recent work on the protein–membrane interaction using liposomes of various compositions.[30,42] Also, the very low concentrations of the surfactant needed to destabilize the protein appear to be relevant for proposing schemes where MG-like states can be induced in physiological systems by compounds like bile salts or hormones with surfactant properties.

Results and Discussion

Conformational changes in BLA induced by micromolar concentration of SDS followed by fluorescence

Increasing the concentration of SDS in the micromolar range affects the fluorescence properties of BLA. At the three pH values investigated, i.e. 4.5, 6.5 and 8.0, the λ_{max} for the fluorescence emission experienced a red shift from 331 nm to 344 nm, characteristic of the MG-state of the protein,[28,43] as the [SDS]/[BLA] ratios are increased from 0 to 25, 0 to 11 and 0 to 65 for each pH value, respectively. Representative fluorescence spectra of BLA in the absence and the presence of 31.4 μM SDS at pH 4.5 are shown in Figure 1(a). For comparison, a spectrum of the protein at 9.9 mM SDS is shown. The progression of the unfolding *versus* [SDS]/[BLA] was monitored as the percentile increase of the fluorescence emission intensity compared to native protein emission (Figure 2(a)), and as the corresponding red shift of the emission λ_{max} (Figure 2(b)). Both curves indicate a cooperative unfolding as the [SDS]/[BLA] ratio increases, at least for pH 4.5 and pH 6.5. The apparent midpoint [SDS]/[BLA] ratios for the conformational transition of the protein at pH 4.5, pH 6.5 and pH 8.0 are 11 μM, 6 μM and 33 μM, respectively. The increase of the fluorescence emission intensity compared to the native protein emission at each pH is 34% (at [SDS]/[BLA]=24), 74% (at [SDS]/[BLA]=10) and 148% ([SDS]/[BLA]=249) for pH 4.5, pH 6.5 and pH 8.0, respectively (Figure 2(a)). At pH 8, the conformational unfolding continues towards higher concentrations of SDS (75 μM), and the shapes of the curves indicate a more generalized, less cooperative unfolding (Figure 2). Denaturation by surfactants such as SDS is generally thought to occur when the hydrophobic parts of the surfactant interact with, and help to expose further, the protein hydrophobic patches, inducing the destabilization of the hydrophobic core of the protein.[31,33,44] There are ways of rationalizing changes in fluorescence intensity into changes in quantum yield (and in turn number of exposed tryptophan residues) and unfolding.[28] Thus, the difference in midpoint concentrations of SDS at the different pH values (Figure 2) may be explained by the exposure of more than one tryptophan residue upon unfolding

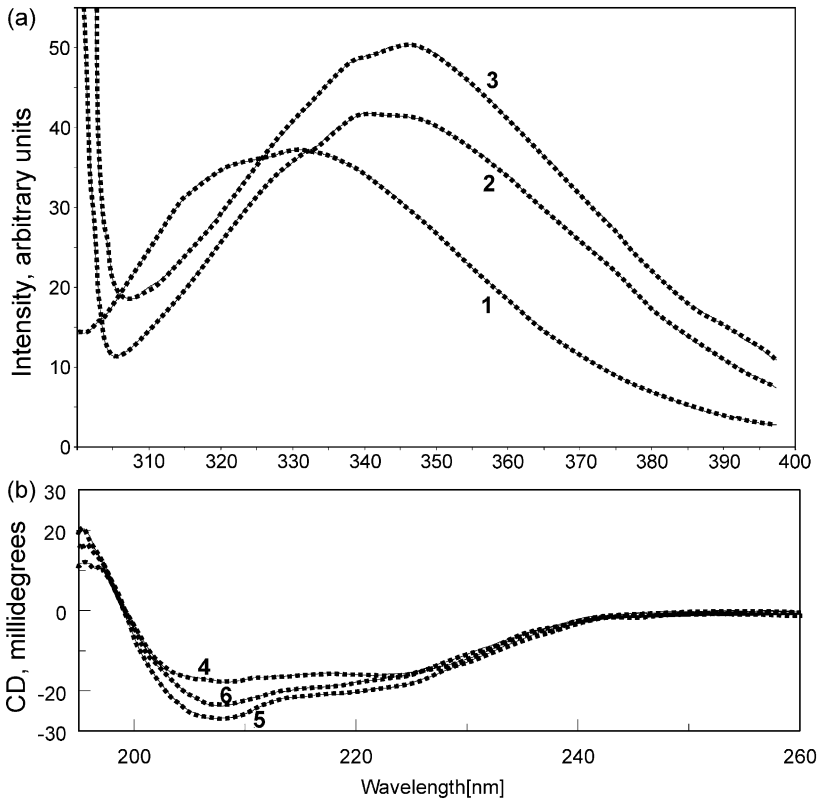

Figure 1. Representative spectra of BLA under native conditions and with different amounts of SDS. (a) BLA examined by fluorescence at pH 4.5. [BLA] = 1.4–1.7 μM. 1, BLA in buffer only. 2, [SDS]/[BLA] = 20, SDS concentration = 31.4 μM. 3, [SDS]/[BLA] = 7018, SDS concentration = 9.9 mM. (b) BLA examined by CD at pH 4.5. [BLA] = 15–17 μM. 4, BLA in buffer only, [BLA] = 17 μM. 5, [SDS]/[BLA] = 20, SDS concentration = 323 μM. 6, [SDS]/[BLA] = 1118, SDS concentration = 17.6 mM.

and differences in quantum yield at the three pH values. Our data suggest that at pH 8.0 there is no stabilization of a distinct intermediate, as is the case at the lower pH values (Figure 2). This is in agreement with the results of other studies, where it has been found that at pH 8 thermal denaturation did not lead to the stabilization of a compact, denatured state of the protein.[45]

To our knowledge, no author has yet reported proteins being partly denatured by micromolar quantities of SDS, as used here with BLA. For comparison, we investigated by fluorescence the response of hen egg-white lysozyme titrated under the same conditions as those used for BLA. As can be seen in Figure 2(a) and (b), no red shift or significant alteration of λ_{max} for the intrinsic fluorescence emission of lysozyme was observed, and the protein appears stable at these conditions. Addition of 8 M urea leads to a pH-dependent red shift in lysozyme.[46] As seen by ANS fluorescence, exposure of hydrophobic areas in this protein is found only when its disulphide bonds are reduced and lysozyme is dissolved in high concentrations of urea or guanidinium chloride (7–10 M).[47]

Conformational changes in BLA induced by SDS followed by CD

We further investigated the titration of BLA with SDS by CD spectroscopy. Representative spectra of the native protein and the protein in the presence of micromolar and millimolar concentrations of SDS are shown in Figure 1(b). BLA shows the characteristic increase in ellipticity accompanying formation of the MG state upon incubation of the protein with a low concentration (150–480 μM) of the anionic detergent at pH 4.5, pH 6.5 and pH 8.0 (Figures 1(b) and 3(a)). The development of ellipticity at 222 nm at each [SDS]/[BLA] ratio at the three pH values is shown in Figure 3(a). Persistent secondary structure is observed at the highest [SDS] (= 17.5 mM; [SDS]/[BLA] = 1118) (Figures 1(b) and 3(a)). The development of ellipticity at 222 nm indicates an increased content of α-helix at higher concentrations of SDS.[23] Further quantitative estimations of α-helix and β-sheet content by neural network calculations using the program CDNN confirmed the trends in the data.[48] Thus, in the absence of SDS the content of α-helix was determined to be around 27% at the three pH values (Figure 3(b)), and increased progressively with surfactant concentration up to 30–31% at 625 μM SDS, [SDS]/[BLA] = 40. At around 8 mM SDS, which coincides with the critic micelle concentration (CMC) for SDS, there appears to be a further increase of helix content of about 1% (Figure 3(b)). These enhancements in content of helix are accompanied by an apparent concurrent decrease in the content of β-sheet (Figure 3(c)). It is tempting to speculate that the stabilization of helical structure by SDS may be related to the interaction of the charged head of the dodecylsulphate molecule with charged key amino acid side-chains. Hence, the surfactant molecules would align along the prospective helix to stabilize exposed hydrophobic side-chains. Previous CD studies by Hamada & Takeda

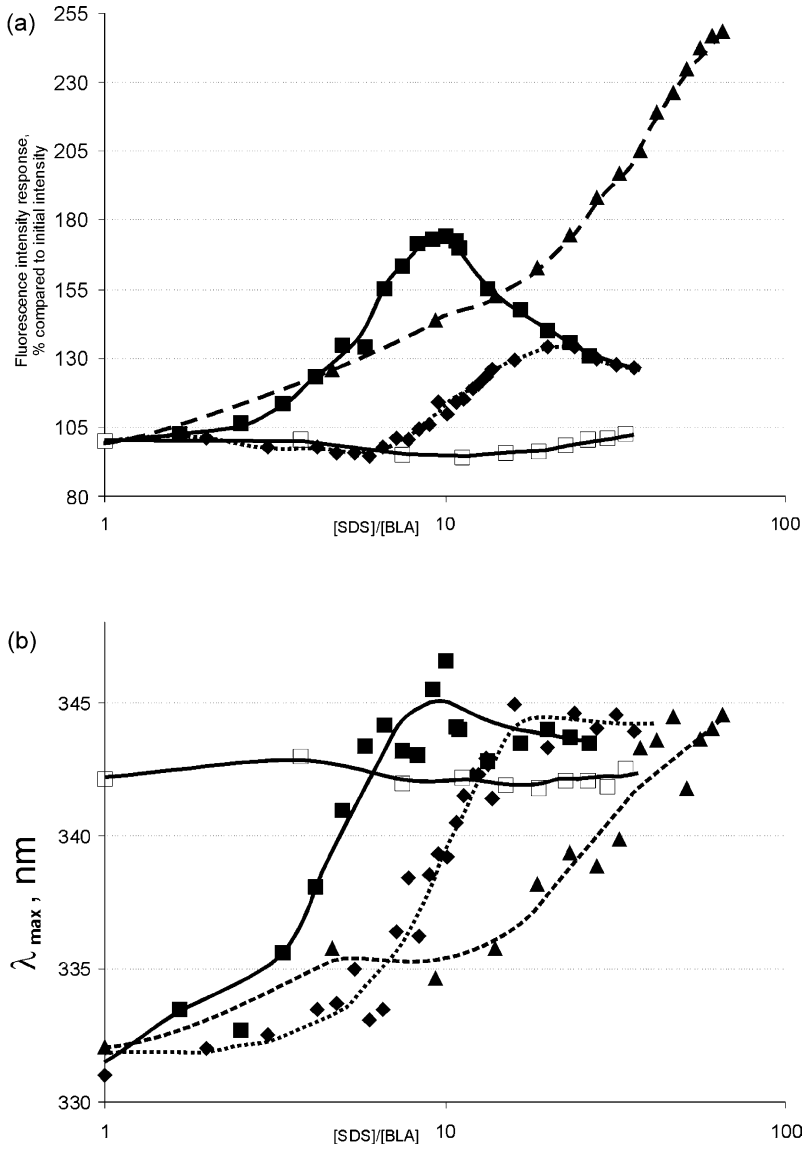

Figure 2. Intrinsic emission fluorescence of BLA and lysozyme at increasing amounts of SDS and at different pH values. Traces are drawn in an arbitrary manner to aid visualization. (a) Fluorescence emission intensity at λ_{max}, relative to emission intensity under native conditions (100%). The *X*-axis scales are on a $\log_{10}$-scale. (b) λ_{max} for the fluorescence emission of BLA. For both (a) and (b): BLA (0.9–1.2 μM) titrated with SDS at pH 4.5 (♦), pH 6.5 (■) and pH 8.0 (▲); lysozyme (0.9–1.2 μM) titrated with SDS at pH 6.5 (□).

have shown that at pH 7, SDS induces the formation of the MG-state of BLA at concentrations >1 mM and [SDS]/[BLA] ratios >40.[34] But in contrast to the results reported by those authors,[34] we could not observe a complete elimination of β-sheet structure at [SDS]/[BLA] ratios ≥400 (Figure 3(c)), although this may be due to methodological differences in secondary structural calculation.

As observed by fluorescence spectroscopy (see above), the midpoints of the titrations are pH-dependent, and at pH 6.5 the protein shows a greater sensitivity towards SDS; in contrast, the titrations monitored by CD are most resistant to change at this pH (Figure 3). Apparently, secondary structural changes occur most easily at non-neutral pH, while the opposite is found for the destabilization of tertiary structure (Figures 2 and 3). In spite of the caveat imposed by the higher ranges of protein concentration required to monitor the effect of SDS by CD than by fluorescence, it appears that at pH 6.5 and pH 4.5 the tertiary conformational changes as observed by fluorescence occur at lower concentrations of SDS than most of the changes in the secondary structure, as measured by CD. At pH 6.5, the unfolding to the intermediate state, as seen by fluorescence, is complete at [SDS]/[BLA]=11, while at this point the secondary structure as seen by CD has changed only a little. At pH 8, however, most changes in secondary structure have occurred at lower [SDS]/[BLA] ratios than those required for the fluorescence intensity to level out. By using CD and at neutral pH, Hamada & Takeda investigated the relation between the secondary (222 nm) and tertiary (270 nm) structural changes in BLA by high concentrations (mM) of SDS,[34] also finding that the apparent extent of unfolding of the tertiary structure appears at lower concentrations of SDS than most of the changes in secondary structure.

Structural calculations by NMR

Many authors have contributed to the characterization of α-LA by NMR; Alexandrescu and

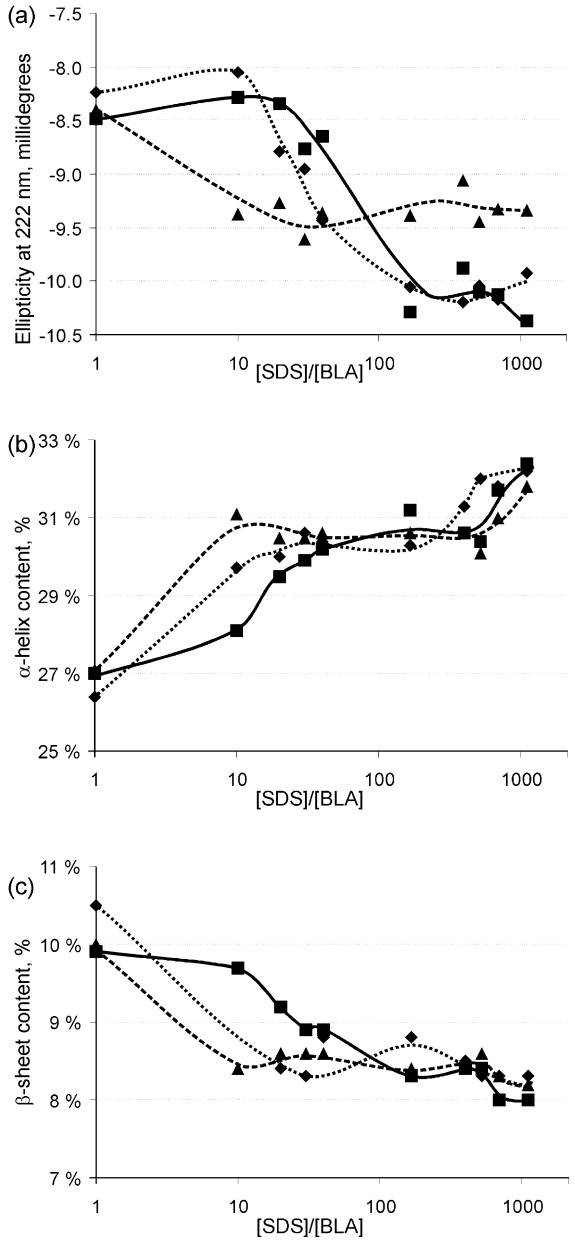

Figure 3. Ellipticity and secondary structure content of BLA at different [SDS] to [BLA] ratios and pH values. (a) Ellipticity at 222 nm. (b) α-Helical content determined by neural network analysis. (c) β-Sheet content determined by neural network analysis. (a), (b) and (c), BLA (15–17 μM) titrated with SDS at pH 4.5 (♦), pH 6.5 (■) and pH 8.0 (▲).

co-workers were early with assignments of aromatic regions of the protein;[49] Kuwajima *et al.* have been cited widely for their work on the MG state,[2] along with the group of Dobson, who has contributed much to the concept of protein folding, using α-LA as a model protein.[41,50] More recently, Redfield *et al*. have contributed with highly detailed works on subtle conformational differences among α-LA species and states.[51,52] Here, we use NMR to provide insights into the fluidity of the structure of BLA under native conditions, under the influence of surfactant molecules and in the presence of micelles.

In order to study BLA interacting with SDS, we first determined the native structure of the protein. Protein labelled with stable isotopes was not used; we attempted to express the recombinant labelled protein primarily by using the expression system described by Grobler *et al.*,[53] which has been used in high-resolution NMR studies.[27] However, we found that the stability of the recombinant protein measured as resistance towards temperature and denaturants was reduced compared to native BLA. This has been shown also by Chaudhuri *et al.*[54] Thus, for this study aiming to elucidate the intrinsic fluidity of the protein and how its conformational stability is influenced by the presence of surfactants, we considered the use of the recombinant protein unsuitable, and used the commercially available protein purified from natural sources (Sigma). Spectral acquisitions were performed at pH 5.6, where the resolution and the signal-to-noise ratio were highest. The data were further analysed by ambiguous restraints for iterative assignment (ARIA), together with chemical shift indexing (CSI), and ^{1}H-^{1}H *J*-coupling constants were analysed by amplitude-constrained multiplet evaluation (ACME).[55–57] Assignments on BLA (Figure 4(a) and data not shown) expanded upon work by Forge *et al.*[27] and Halskau *et al.*[42] Of the 120 backbone amide protons and 129 H^{α} in the protein, 116 and 119 have been assigned, respectively. The spin systems of 90 of the residues have been completely, or almost completely (more than 80%), assigned. Assigned spectra and assignment tables are available upon request.

The calculation in the final ARIA iteration used 2178 nuclear Overhauser effect (NOE) restraints, 625 of which were ambiguous. There were approximately 900 non-redundant, long-range restraints. Of the 20 structures calculated, the lowest-energy structure violated 222 of the NOE restraints, 15 of these violations were larger than 0.3 Å. The seven lowest-energy structures are superimposed and presented in Figure 5(a). The lowest-energy structure (Figure 5(b)) also violated 27 of the 130 dihedral restraints derived from CSI and 9 of the 44 coupling constant restraints. The RMSD for all the atoms included in the seven structures (Figure 5(a)) and for backbone atoms are plotted against residue number in Figure 5(c). The N and C-terminal regions of the protein show high RMSD. The highest RMSD value, i.e. 8.3 Å, was measured for the N-terminal residue, E1. The most unstructured region is the C terminus, almost all the residues from K108 to L123 have RMSD for the backbone atoms >1.0 Å. In addition to the N and C-terminal regions, there are three other regions in the protein with RMSD >1.0 Å, i.e. residues 17–19, 37–52 and 62–71. The average RMSD for the backbone atoms of all residues is 1.3 Å. When including the side-chains, the average RMSD is 1.8 Å but these values are reduced to 1.0 Å (backbone atoms) and 1.4 Å (all

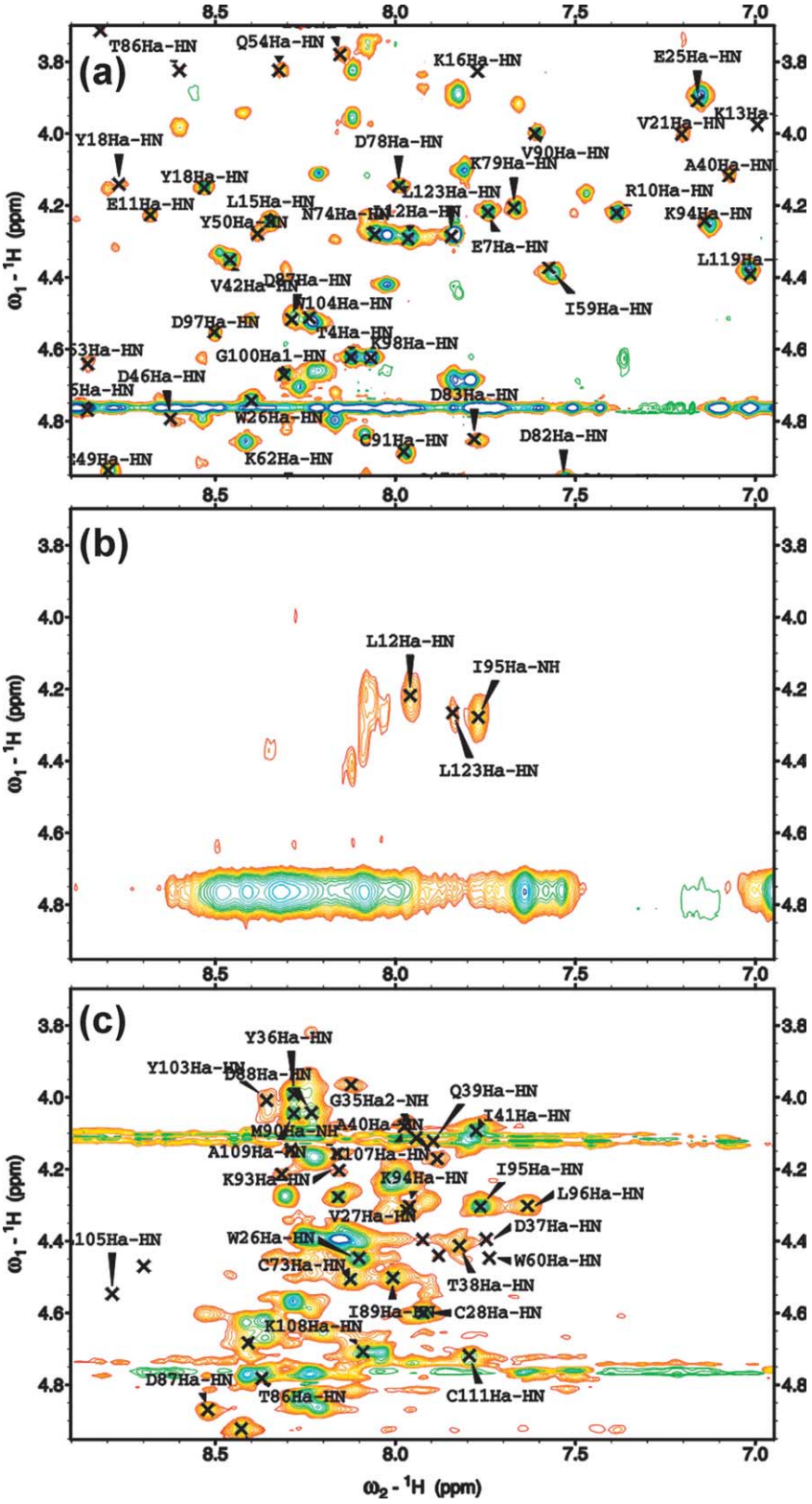

Figure 4. Fingerprint regions of TOCSY spectra of BLA at pH 6.5 and 310 K. (a) Native state of BLA. Spectrum taken at pH 6.5 (similar spectra are recorded at pH 5.6). (b) BLA at critical point, where very few crosspeaks are detectable, [SDS]/[BLA]=5.2, pH 6.5. (c) BLA bound to surfactant micelles, [SDS]/[BLA]=43, pH 6.5.

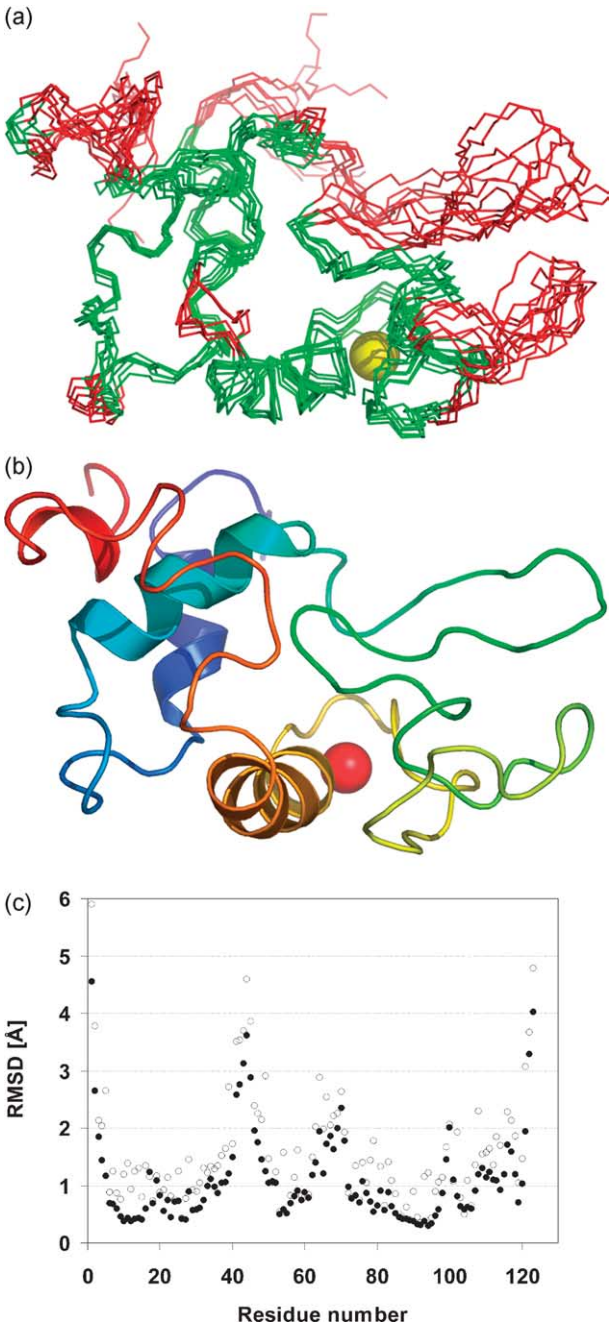

Figure 5. Structural calculation of native BLA at pH 5.6 and 310 K. (a) Superimposition of the seven lowest-energy structures of the 20 calculated structures. Residues with backbone atoms with RMSD < 1.0 Å are coloured green, while those with RMSD > 1.0 Å are in red. (b) The structure of lowest energy. (c) Plot of the backbone RMSDs (●) and the mean RMSD of all atoms in each residue (○).

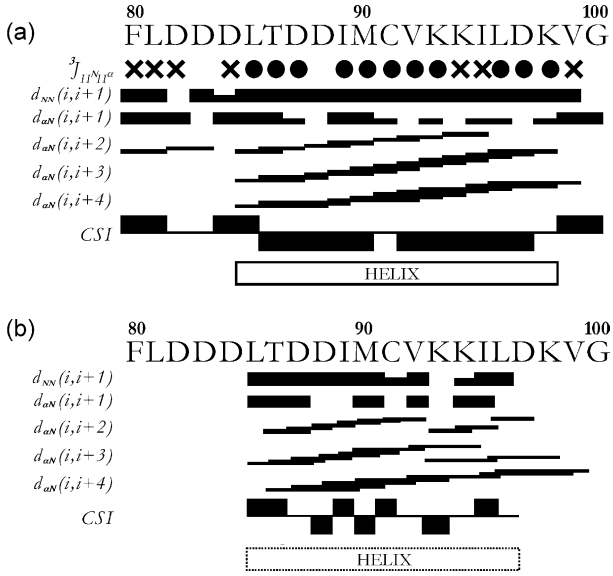

Figure 6. Secondary structure assessment of residues 80–100 using $^{3}J_{H^{N}H^{\alpha}}$ coupling constants, $d_{NN}(i,i+1)$, $d_{N\alpha}(i,i+1)$, $d_{N\alpha}(i,i+2)$, $d_{N\alpha}(i,i+3)$ and $d_{N\alpha}(i,i+4)$ NOE connectivities and CSI. (a) Data derived from NMR experiments on BLA at pH 5.6 and 310 K. (b) Data derived from NMR experiments on BLA at pH 6.5 and 310 K in the presence of SDS at [SDS]/[BLA] = 43.

atoms) when excluding the poorly defined terminals (residues 1–5 and 108–123). A Table with the structural statistics is included as Supplementary Data. The average RMSD for the well-defined C-helix is 0.4 Å (backbone atoms) and 0.7 Å (all atoms) (Figures 5(c) and 6(a)).

The low quality of the structure, especially near the termini, might reflect the need for more restraints and/or the inherent flexibility of the water-soluble structure. The regions with the highest RMSD values appear to correspond well with regions of high *B*-factors reported for the X-ray structures of BLA,[58,59] which lend support to the notion that the structure is at least qualitatively reliable. The CSI of the entire protein predicts only 73% of the secondary structure to be similar to that in the X-ray structure. This is lower than the expected 90–95% accuracy of this method,[57] and might indicate a fluctuating structure. An excerpt of NOE connectivities, CSI and $^{3}J_{H^{N}H^{\alpha}}$ characteristic for secondary structure is presented in Figure 6(a). As can be seen, the C-helix (residues 86–99) cannot be predicted correctly from the CSI alone. Moreover, residues 99–101 and 110–113 appear to contain β-sheets according to CSI, and are flexible (Figure 5(c)). While there is little reason to believe that this is in fact the case, the inability of CSI to characterize this region correctly might reflect the protein ability to attain multiple states in response to changes in conditions. Indeed, the K114N mutation stabilizes the 110–113 region and at the same time interferes with the function of BLA.[60,61] An X-ray structure of the lactose synthase complex shows that the aforementioned region is in close contact with its substrate galactosyltransferase.[62] Other residues contacting the galactosyltransferase are E2, V42 and D44. These three residues are located on parts of the chain that have great flexibility according to the *B*-factors from the crystal structure,[59] and from the RMSD values found in this study. This may suggest that the flexibility of

these residues is important also for the lactose synthase function.

The most prominent difference between the calculated structure and the X-ray structure reported by Chrysina *et al*. [58] is the lack of structural information on the cleft region (involving residues F31, H32, Y103 and I110, among others). This region has been reported to be important for the lactose synthase complex function.[60] No NOE was found across this putative structural feature, which may account for much of the uncertainty in the reported NMR-structure.

Transition from native to SDS-bound state followed by NMR

SDS titration monitored by NMR total correlated spectroscopy (TOCSY) spectra showed a general decrease in native state crosspeak volumes; titrations were performed at pH 6.5, since according to the fluorescence studies, the protein displayed greatest sensitivity towards SDS at this pH (Figure 2). The behaviour of representative H^{α}-H^{N} crosspeaks is shown in Figure 7. At a [SDS]/[BLA] ratio of 5.2 (the critical ratio) no native state crosspeaks could be discerned with certainty, and the fingerprint area appeared to be largely empty (Figure 4(b)). The critical [SDS]/[BLA] ratio is invariant for different absolute concentrations of BLA ranging from 0.9 mM to 1.7 mM (data not shown). This critical point corresponds well with the ratio at the midpoint for the fluorescence titration at pH 6.5 (Figure 2). Only the H^{α}-H^{N} crosspeaks for L12, I95 and L123 could be tentatively assigned (Figure 4(b)). The crosspeaks assigned as L12 and L123 correspond very closely to the shifts these resonances display in the native state; I95 corresponds to the MG-like state discussed below. The other crosspeaks show no clear correspondence to either the native or the MG-like state, but have spin systems consistent with aliphatic residues. It is, however, very difficult to assign these, due to the very poor quality of the spectra at these conditions. Further increase in SDS concentration caused the gradual reappearance of crosspeaks in the fingerprint area, with chemical shift dispersion consistent with an MG-like state (Figure 4(c)), apparently similar to the TFE state.[24]

It seems likely that single SDS molecules interact with BLA in a largely unspecific manner, making available conformations and new binding sites as the unfolding proceeds. At [SDS]<CMC this system seems unsuitable for NMR observations. At [SDS]>CMC, the TFE-acid-like state is stabilized probably by sequestering of BLA towards the negative micelles. Much work on MG-like states of BLA exists; lately, there have appeared a number of papers concerning the MG-like state of BLA bound to oleic acid, named HAMLET, since this state is associated with the selective apoptosis of cancer cells.[63,64] This has led to attempts to localize the binding site of the oleic acid molecule.[65] But, although important progress has been made towards characterizing and observing directly MG-like states of BLA by NMR,[22,27,52] a structural characterization of the HAMLET state, including the residue-specific identification of the oleic acid-binding site, has not been reported by NMR. Oleic acid does not interact directly with holo-BLA, which requires a degree of unfolding to bind,[64,66] complicating the monitoring of a gradual binding of the acid. It is possible that the SDS titrations presented here mimic the oleic acid binding, as the two molecules resemble each other. The SDS molecules would first weaken the tertiary structure of the protein by unspecific interactions, exposing

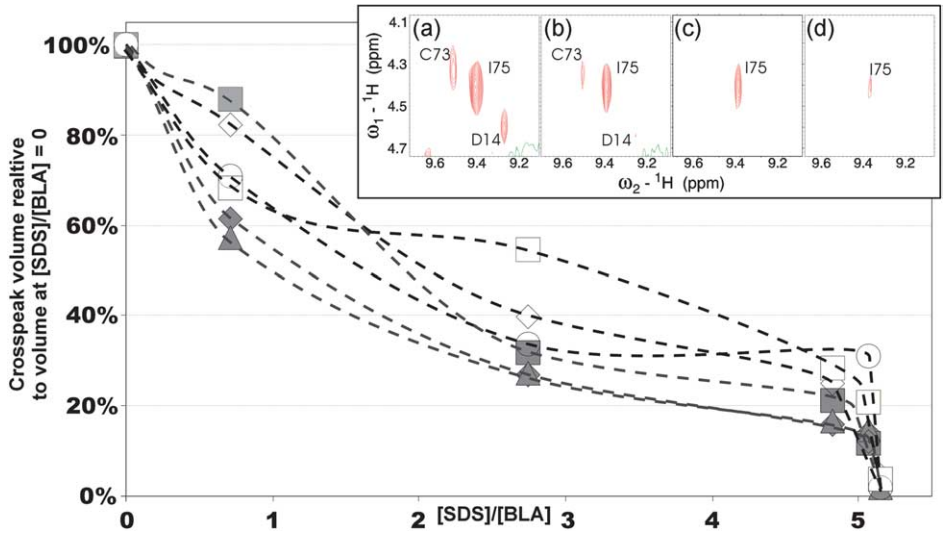

Figure 7. Selection of H^{α}-H^{N} crosspeak integral volume behaviour with increasing amounts of SDS at pH 6.5. The values are shown relative to the crosspeak volumes for BLA at [SDS]/[BLA]=0 (100% crosspeak volume) for residues K79 (□), R10 (◇), D14 (○), I75 (▣),V99 (◆) and E49 (▲). The traces are drawn in an arbitrary manner to aid visualization. Insets (a)–(d), Screenshots from TOCSY spectra processed by Sparky showing crosspeak behaviour at [SDS] to [BLA] ratios of (a) 0:1, (b) 2.74:1, (c) 4.82:1 and (d) 5.07:1.

the binding site. However, this putative state also appeared to be unobservable by the NMR experiments attempted here (Figure 4(b)), possibly due to a large number of populated states fluctuating at the intermediate NMR timescale or a tendency towards aggregation of several protein molecules. Indeed, the apoptosis-active HAMLET has been reported to be multimeric.[63] Casbarra *et al.* have recently probed the binding site of oleic acid in HAMLET by hydrogen/deuterium exchange and limited proteolysis experiments coupled to mass spectrometry analysis.[67] The authors propose that the carboxyl moiety of oleic acid might replace the interactions of β-COOH of D37 and form a salt-bridge with the N-terminal lysine residue (K1) of human α-LA, destabilizing the β-sheet region.[67] Another assumption, which is more consistent with a mechanism for BLA and its tumour apoptotic form BAMLET,[66] where K1 from HAMLET is not conserved (i.e. replaced by E1), is that oleic acid interacts with other positively charged residues. For instance, interaction with K58, at the C-terminal end of the three β-sheet strands, could disrupt the salt-bridge between this residue and D46, contributing to destabilize the β-domain. This part of the protein is reported to be less stable than the α-domain,[22,51] and its conversion to helices upon partial denaturation has been described or theorized.[34,68] At pH 6.5, the protein has a net negative charge, and stabilizing coulombic contributions will be countered partly by the predomination of negative charges repelling each other. Screening of positive charges on the protein surface by the surfactant will aggravate this feature. This trend continues towards higher pH values (Ø.H. *et al.*, non-published data), which may explain the lower resistance to SDS denaturation at pH 6.5 and pH 8.0 than at pH 4.5, as seen by fluorescence (Figure 2).

BLA bound to dodecylsulphate micelles

Assignments on the SDS-state included 37 of the H^{α}-H^{N} crosspeaks and some of their side-group protons. The overall shift-values resemble those for the acidic TFE state, and the assignment procedure relied initially on the work of Alexandrescu *et al.* on this state (Table 1).[24] In fact, of the 60 backbone H^{α} and H^{N} chemical shifts compared, 49 deviated less than 0.1 ppm from their corresponding resonances in the TFE state (Figure 4(c) and data not shown).[24] This semblance is noteworthy, considering that in our work the bulk conditions are pH 6.5 and pH 4.5 in buffered water, and it is likely that the observed conformer is BLA sequestered from the bulk solution and interacting closely with micelles. In contrast, the tryptophan side-chain resonances show larger deviations in chemical shift compared to the TFE state, of the order of −0.4 to 0.4 ppm (Table 2). This observation might conceivably be explained by a partial orientation of these large, aromatic residues with respect to the micelle. Such an individual side-chain orientation would be possible in the flexible, MG-like state of the micelle-associated protein. In this scheme, one end of the side-chain would spend more time in close association with the micelle compared to the other end. In an isotropic solution, such local orientations would not occur. Tryptophan residues are well known to impart large, stabilizing enthalpic contributions to the free energy of the protein–membrane systems.[69,70]

The majority of the assigned resonances in the spectrum for the micelle-bound protein was found in the vicinity of the C-helix, regarding the native structure, where $d_{NN}(i,i+1)$ and other NOE connectivities characteristic for α-helical structure could be found (Figure 6(b)). Similar, but not as complete, connectivities could be found also for residues G35–I41 and Y103–A109. These observations correspond well with work by Alexandrescu *et al.* on the TFE/low pH-induced state of BLA.[24] As also described by those authors, we encounter strong overlap problems and many crosspeaks seem attenuated or missing altogether. Alexandrescu *et al.* make a distinction between the TFE-induced conformation and the acid-MG, alleging differences in ANS binding and linewidth. Also, the helical propensity of the region G35–I41 is reported to be non-native. This region is also reported to form non-native helical structure in a high-temperature examination of the BLA MG state.[52] When comparing the NMR data for the C-helix at pH 5.6 in the native and SDS-bound states (Figure 6), the tendency to form a stable helix in the micellar state is much lower than in the native state, as seen by CSI and completeness of $d_{NN}(i,i+1)$ and $d_{\alpha N}$ NOE interactions. Considering the helical increase reported by CD (Figure 3), this appears contradictory. However, while non-native helical structure may be induced, the NMR detectable hydrogen bonding network is not necessarily stable enough to give helical NOE-patterns and consistent CSI values. Indeed, due to random-coil to helical structural fluctuations, crosspeaks from such regions may be attenuated severely due to chemical exchange broadening. Thus, NMR may underreport helical structure in some instances, especially when the protein exists in intermediate folding states, as is the case here for BLA. However, fluctuating helical structure might still contribute to increased ellipticity when the system is examined by CD, since this method will reflect the chirality in an average of conformations. Conversely, the large C-helix appears to be weakened; this feature is common for MG-like states and is supported by ^{1}H exchange studies.[22]

Conclusions

BLA is sensitive to very small amounts of dodecylsulphate anions, which partly denature the protein. At [SDS] > CMC, the partially unfolded protein binds to the negatively charged micelles. We suggest a model including pH-modulated equilibria between BLA, BLA bound to multiple

Table 1. Assignments of BLA in the presence of SDS micelles, 78 mM SDS at pH 6.5 and 310 K (values in ppm)

Residue	H^N	H^α	$H^{\beta1/\beta2(\beta3)}$	Others
W26	8.11	4.42	3.56	$H^{\delta1}$=7.39; $H^{\varepsilon1}$=10.11; $H^{\varepsilon3}$=7.53; $H^{\zeta2}$=7.52; $H^{\zeta3}$=6.83; $H^{\eta2}$=7.12
V27	7.96		1.93	$H^{\gamma1/\gamma2}$=0.86
C28	7.90	4.59	2.93/3.03	
S34	8.08			
G35	7.95	$H^{\alpha1/\alpha2}$=4.07/4.10		
Y36	8.29	3.99	2.87/4.67	$H^{\varepsilon1/\varepsilon2}$=6.83; $H^{\delta1/\delta2}$=7.21
D37	7.76	4.39		
T38	7.84	4.40	4.22	H^{γ}=1.81
Q39	7.83	4.15		
A40	4.16	7.88		
I41	4.11	7.76		
W60	7.75	4.45	3.42	$H^{\delta1}$=7.30; $H^{\varepsilon1}$=10.06; $H^{\varepsilon3}$=7.49; $H^{\zeta2}$=7.50; $H^{\zeta3}$=6.87; $H^{\eta2}$=7.50
H68		4.86		$H^{\delta2}$=8.70; $H^{\varepsilon1}$=7.50
C73	8.11	4.50		
L85	8.74	4.63		
T86	8.35	4.81		
D87	8.53	4.86	3.32/3.45	
D88	8.21	4.05		
I89	8.00	4.47		
M90	8.15	4.15		
C91	8.41	4.91		
V92	7.89	3.96		
K93	8.16	4.18		
K94	7.92	4.27		
I95	7.75	4.31		
L96	7.58	4.28		
V99	8.54	4.56		
G100	8.07	$H^{\alpha1/\alpha2}$=3.80		
Y103				$H^{\delta1/\delta2}$=6.82; $H^{\varepsilon1/\varepsilon2}$=6.93
W104	8.43	4.15	3.37/3.49	$H^{\delta1}$=7.38; $H^{\varepsilon1}$=10.13; $H^{\varepsilon3}$=7.62; $H^{\zeta2}$=7.55; $H^{\zeta3}$=6.85; $H^{\eta2}$=7.21
L105	8.77	4.52		
A106	8.19	4.46		
H107	7.98	4.08	3.02/3.25	$H^{\delta1}$=7.21; $H^{\varepsilon1}$=8.43
K108	8.07	4.71	3.36/3.44	
A109	8.29	4.04	1.37	
C111	7.78	4.69	3.18/3.32	
W118				$H^{\delta1}$=7.25; $H^{\varepsilon1}$=10.24; $H^{\varepsilon3}$=7.64; $H^{\zeta2}$=7.62; $H^{\zeta3}$=6.85; $H^{\eta2}$=7.10

dodecylsulphate ions, BLA interacting with micelles and BLA being denatured at high concentrations of SDS (Figure 8). The model summarizes the qualitative features of the fluorescence data. The protein secondary structure also responds in a dose-dependent manner, and the two responses are likely co-dependent. Weakening of tertiary structure seems to increase the susceptibility of the protein towards these changes, except at pH 8, where the data support a more generalized unfolding without stabilization of an intermediate folding state. The [SDS]/[BLA] ratios at which the transition from native to MG-like state occurs are pH-dependent, with midpoints for pH 4.5 and pH 6.5 of about 11–12 and 6, respectively (Figure 2). The concentration at which the transition from the MG state to the micelle-associated state occurs is likely a function of the pH, the amount of BLA present and the CMC of SDS at these conditions. It is difficult to quantify this transition from the available data, but we note that at an [SDS]/[BLA] ratio of about 35 and 1.8 mM BLA there appears to be no further crosspeak intensity increase upon addition of more SDS at pH 4.5. However, at this

Table 2. Comparison of the SDS-micellar state studied in this work and the TFE-acid state[63]

Residue	$\Delta H^{\delta1(\delta2)}$	$\Delta H^{\varepsilon1}$	$\Delta H^{\varepsilon3}$	$\Delta H^{\zeta2}$	$\Delta H^{\zeta3}$	$\Delta H^{\eta2}$
W26	−0.17	−0.28	−0.04	−0.07	0.26	0.8
W60	−0.08	−0.30	0.14	−0.06	0.27	−0.31
W104	−0.06	−0.25	0.04	−0.03	0.22	0.02
H107	0.15	0.42	NA	NA	NA	NA
W118	−0.02	−0.38	−0.05	−0.15	0.23	0.09

Δ-Values (in ppm) are calculated as $\Delta H^x = \delta_{TFE} - \delta_{SDS}$, where x is δ1, δ2, ε1 or η2. $H^{\delta1(\delta2)}$, the (δ2) applies to H107. NA, not applicable.

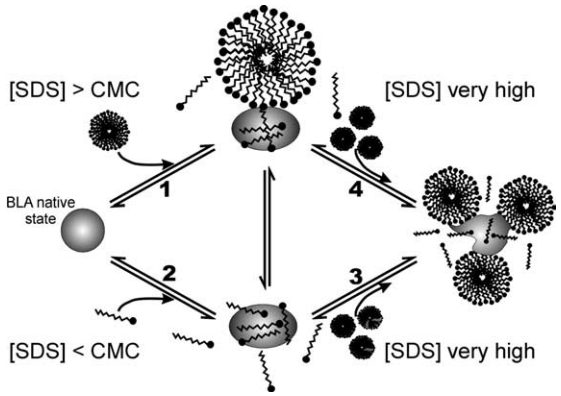

Figure 8. Schematic summary of SDS-induced states of BLA. Equilibrium (1): above the CMC, the protein may interact directly with the membrane-mimicking micelles. Under the current conditions, there will be negligible amounts of native protein available for this interaction, as there will be high levels of unaggregated surfactant molecules available that partly denature the protein. Equilibrium (2): the equilibrium is influenced by pH, and it is shifted towards the surfactant-associated state at neutral pH compared to lower pH. Equilibriums (3) and (4): transitions to the denatured protein; the direct transition to a general unfolding appears to be more efficient at higher pH. See the text for a quantitative description of concentrations and [SDS]/[BLA] ratios for the transitions.

[SDS]/[BLA] ratio but pH 8.0, the protein appears to denature instead of being stabilized by the micelles. The protein is eventually denatured at all pH values at molar concentrations of SDS leading to a form with $\lambda_{max}=353$ and quenched fluorescence (data not shown).

The very low level of surfactant necessary to affect the folding state of the protein is noteworthy. The immediate consequence of this observation is that very low concentrations of some compounds may alter the folding state of certain proteins. Indeed, we propose that such sensitivity towards surfactants should be found in all proteins exhibiting a propensity to form a stable MG state. Some other relevant proteins, such as cytochrome *c* and beta-lactoglobulin are reported to form a stable MG-state in the presence of millimolar quantities of surfactants.[7,32–34,44] The sensitivity towards denaturation and the exact properties of the resulting compact denatured state may conceivably be modulated by the specific nature of the surfactant, as indeed has been reported for cytochrome *c*.[33] Also, the oleic acid reported to be a necessary cofactor of HAMLET, while having a reasonable resemblance to the SDS surfactant, does not interact directly with native BLA.[64,66] It is possible that the intermediate state at [SDS]/[BLA]≥5 contains conformers of the protein that mimic the HAMLET state, in which the initial unspecific surfactant interactions provide the unfolding necessary for the cofactor binding site to be exposed. This unfolding cannot be initiated by oleic acid, as very little non-micellar fatty acid is available in solution. Also, dodecylsulphate molecules will always be negatively charged at pH>1, while oleic acid has a pK_a of about 4.5.

Thus, the findings reported and cited here suggest that *in vivo* there might be an increased likelihood of formation and stabilization of MG states due to the presence of physiological surfactants. These MG states have been implicated in both healthy and pathological processes; they are reported to be precursors for formation of amyloid plaque, characteristic for the ailments Alzheimer's disease and bovine spongiform encephalopathy.[9,71] On the other hand, the MG state is also thought important for the function of many proteins.[12,32] Thus, there might be only subtle differences that discern a healthy and a pathological state derived from MG-prone proteins.[9] For instance, there have been reports on specific metal ions and pH conditions triggering and aggravating the formation of β-amyloid plaque.[71,72]

Finally, the micelle-bound state (this work) and the low-pH/TFE-induced state of BLA,[24] as probed by NMR, appear to be rather similar. Both TFE and micelles are used as membrane-mimicking media, and allow direct and simple ways of examining how proteins may behave in association with membranes. In two earlier studies, we have characterized a detailed mechanism for BLA interacting with negatively charged membranes and the possibility for this bound state to be modulated by the phospholipid content of the model membranes.[30,42] The residue-level specificity of the work was achieved using NMR-monitored ^{1}H–^{2}H exchange techniques. Thus, the structural picture of the membrane-bound state of BLA was indirect. The micelle-bound state of BLA might represent a more direct observation of a state analogous to the membrane-bound BLA, although its fluorescence properties indicate some differences, i.e. the state appears more red-shifted than the liposome-bound conformer and its emission intensity varies with pH.[23,29,30,40] It is likely that the strong pH gradient initiates the first step of the association by protonating key acidic residues, making the protein eligible for coulombic attraction towards the negatively charged micelle. However, the closer and possibly more specific association where hydrophobic side-chains partition into the amphitropic aggregate, as supposed in the unilamellar vesicles and other biological membranes, does not happen in the SDS micelles.[35,73] The reason for this may be the curvature of the micelle, the presence of single dodecylsulphate molecules that stabilize the intermediate state or the lack of stable hydrophobic patches on the micelle surface. Yet, it is noteworthy that the C and A-helices, which are exchange-protected and involved in binding to negatively charged liposomes,[42] are preserved in the SDS micelle-bound state, and these states resemble each other when examined by CD.[30,42] Thus, although micelles have limitations and drawbacks as membrane-mimicking systems,[35] they remain a

reasonable choice for NMR structural and dynamic studies of biological macromolecules, since the more physiologically relevant liposomes have too slow tumbling rates for high-resolution NMR. Examination of SDS micelles has provided useful insights for some important membrane-associating proteins, such as cytochrome *c*[32] and α-synuclein.[74] We propose that structural features of the micelle-bound state described here, as well as the rather similar TFE state,[24] appear to reproduce the membrane-bound state, still showing dynamical and structural differences from the acid MG. Bychkova *et al*. predicted earlier that physiologically relevant MG states were connected to membrane interfaces,[75] and these findings vindicate their proposal.

Materials and Methods

Calcium-bound bovine α-lactalbumin (BLA), hen egg-white lysozyme, both lyophilized powder at 85% and 95% purity, respectively, sodium dodecylsulphate (SDS) and ^2H_2O of 99% purity were acquired from Sigma.

Fluorescence measurements

Fluorescence measurements were performed on a Perkin-Elmer LS-50 spectrometer. Samples were prepared at pH 4.5 in 20 mM citric acid/Na_2HPO_4 buffer, 0.1 M NaCl, and at pH 6.5 and pH 8.0 in 100 mM KH_2PO_4/K_2HPO_4 buffer. BLA or lysozyme were added to the cuvette at the indicated concentrations and SDS from stock solutions was added sequentially and directly to the fluorescence cuvette with rapid mixing, so that the concentration of SDS ranged from 1 μM to 25 mM. Fluorescence emission experiments were performed for each concentration of SDS with excitation at 295 nm and emission scan range from 310 nm to 400 nm. The cuvette was kept at 310 K by flow-through temperature control. Data were acquired for the same SDS concentration range in the absence of BLA and background SDS-only spectra were subtracted from spectra acquired from BLA-containing samples at corresponding concentrations of SDS. The emission of buffer and SDS was negligible at the emission maximum of lysozyme. The resulting datasets were treated with a moving average data handling option consisting of 15 data points. For emission intensity data, the values were adjusted by volume effects, assuming a simple linear relation between emission intensity and concentration of BLA or lysozyme in the range 0.9–1.2 μM. Emission intensity data were also normalized to adjust for variations in the initial amount of added BLA stock solution.

CD measurements

CD measurements were performed on a Jasco J-810 spectropolarimeter. Sample series were prepared at pH 4.5, pH 6.5 and pH 8.0 at concentrations of BLA of 15–17 μM and progressively increasing amounts of SDS were added directly into the cuvette. Spectra were acquired at 310 K with a scan speed of 100 nm/minute and response of two seconds. Four scans were accumulated and averaged, and blanks were subtracted for each concentration. Volume effects on BLA concentration were tracked and adjusted for. Secondary structure content was estimated by neural network analysis performed using the program CDNN developed by Bohr *et al*.[48]

NMR measurements

All spectra were acquired at 314 K on a Bruker Avance DRX 600 spectrometer employing a probehead with inverse (1H) detection and *x*, *y*, *z*-gradient coils.

Assignment of the native state of BLA

Samples contained 1.6 mM BLA in 550 μl of H_2O and 50 μl of ^2H_2O phosphate/citric acid buffer, adjusted to pH 5.6. NOESY spectra with mixing times of 30 ms, 60 ms, 90 ms, 120 ms and 150 ms were acquired using 576 and 4000 time domain points in *F*1 and *F*2, respectively. The number of scans was 64, and a water flip-back pulse was used to reduce radiation damping of the strong water-signal.[76] A Gaussian shaped pulse was employed with a pulse-length of 10 ms. A gradient selective-DQF-COSY[77] experiment using 640 and 4000 time domain points in *F*1 and *F*2, respectively, was acquired. The number of scans was 56. A TOCSY spectrum was acquired with 768 and 1000 time domain points in *F*1 and *F*2, respectively, 64 scans and a spin-lock mixing time of 80 ms.

Assignment of the SDS-states of BLA

Samples contained 1.8 mM BLA and 78 mM SDS in 300 μl of H_2O and 20 μl of ^2H_2O buffered at pH 4.5 in a Shigemi-type sample tube (Shigemi Inc.). TOCSY and NOESY experiments were acquired using 85 ms and 80 ms mixing times, respectively. The TOCSY spectrum employed 512 and 1000 time domain points in *F*1 and *F*2, respectively, and 48 scans. The NOESY spectrum was acquired with 512 and 2000 time domain points in *F*1 and *F*2, respectively and 56 scans.

Acquisitions for NMR-monitored SDS titrations

Samples for SDS titrations typically consisted of BLA in the range of 0.9–1.0 mM. Titrations covered two ranges of SDS concentrations, 0–8.8 mM and 8.9–31.0 mM. These concentrations gave [SDS]/[BLA] ratios in the range of 0–5.6 and 4.7–43.1 for the examination of SDS–BLA interactions at ratios in the range of, and beyond, the cooperative unfolding shown by fluorescence. The titration in the 0–5.6 range was performed buffered at pH 6.5; the titration in the 4.7–43.1 range was performed at both pH 4.5 and pH 6.5 to see if the micelle-associated state responded differently to titration at the two pH values. Two TOCSY techniques were used: the regular TOCSY and band-selective homonuclear decoupled (BASHD)-TOCSY.[78] Typical acquisition parameters for TOCSY experiments were: number of scans 96, time domain points in *F*1 and *F*2, 128 and 2000, respectively, and spin-lock field mixing time of 50 ms. Typical acquisition parameters for BASHD-TOCSY were: number of scans 96, time domain points in *F*1 and *F*2, 32 and 2000, respectively, and mixing time of 50 ms. Spectra with mixing time of 95 ms were acquired to transfer magnetization towards protons at the extreme ends of residue spin systems, for clarification of assignments.

Unless otherwise specified, water suppression was achieved using the double pulse field gradient spin echo (excitation sculpting) modification of the Watergate suppression scheme.[79]

Structural calculations

The 3D structure of BLA was calculated using the ambiguous restraints for iterative assignments software (ARIA v1.2)[56] and the Crystallography & NMR system (CNS v1.1).[80] The input for the structural calculation was a partially assigned peak list consisting of 4101 peaks. This list had been generated automatically by automated peak picking for NMR spectroscopY software package (AUTOPSY)[81] from a NOESY-type spectrum with a mixing time of 150 ms. Further constraints used in the structural calculations were provided by $^{3}J_{H\alpha HN}$ coupling constants and secondary structure assessments.[82] Coupling constants were derived from a phase-sensitive COSY experiment employing presaturation for water suppression and using the amplitude constrained multiplet evaluation (ACME) software.[55] The CSI method for determining secondary structure from chemical shift data was used.[57] Residues that according to CSI were located in α-helices or β-sheets were given φ-angles and ψ-angles of −57° and −47° or −139° and 135°, respectively. The Ca^{2+}–O atom distances were restrained to 2.4(±0.2) Å. The BLA correlation time was set to 10 ns. The template file was based upon the crystal structure of BLA, 1F6S.pdb.[58] Protons were also added to the three histidine residues to reflect their protonated state at pH 5.6. The simulated annealing and cartesian molecular dynamics procedures were performed using CNS.

Acknowledgements

This work was supported by The Research Council of Norway. We are very grateful to Professors Holm Holmsen and Arturo Muga for valuable discussions.

Supplementary Data

Supplementary data associated with this article can be found, in the online version, at doi:10.1016/j.jmb.2005.04.020

References

1. Arai, M. & Kuwajima, K. (2000). Role of the molten globule state in protein folding. *Advan. Protein Chem.* **53**, 209–282.
2. Kuwajima, K. (1996). The molten globule state of alpha-lactalbumin. *FASEB J.* **10**, 102–109.
3. Ptitsyn, O. B. (1995). Molten globule and protein folding. *Advan. Protein Chem.* **47**, 83–229.
4. Englander, S. W. (2000). Protein folding intermediates and pathways studied by hydrogen exchange. *Annu. Rev. Biophys. Biomol. Struct.* **29**, 213–238.
5. Bychkova, V. E., Dujsekina, A. E., Klenin, S. I., Tiktopulo, E. I., Uversky, V. N. & Ptitsyn, O. B. (1996). Molten globule-like state of cytochrome c under conditions simulating those near the membrane surface. *Biochemistry*, **35**, 6058–6063.
6. Torta, F., Dyuysekina, A., Cavazzini, D., Fantuzzi, A., Bychkova, V. & Rossi, G. (2004). Solvent-induced ligand dissociation and conformational states of cellular retinol-binding protein type I. *Biochim. Biophys. Acta*, **1703**, 21–29.
7. Uversky, V., Narizhneva, N., Kirschstein, S., Winter, S. & Lober, G. (1997). Conformational transitions provoked by organic solvents in beta-lactoglobulin: can a molten globule like intermediate be induced by the decrease in dielectric constant? *Fold. Des.* **2**, 163–172.
8. Epand, R. M. & Kraayenhof, R. (1999). Fluorescent probes used to monitor membrane interfacial polarity. *Chem. Phys. Lipids*, **101**, 57–64.
9. Uversky, V. & Fink, A. (2004). Conformational constraints for amyloid fibrillation: the importance of being unfolded. *Biochim. Biophys. Acta*, **1698**, 131–153.
10. Dobson, C. M. (2003). Protein folding and disease: a view from the first Horizon Symposium. *Nature Rev. Drug Discov.* **2**, 154–160.
11. Demchenko, A. P. (2001). Recognition between flexible protein molecules: induced and assisted folding. *J. Mol. Recogn.* **14**, 42–46.
12. Dunker, A. K., Brown, C. J., Lawson, J. D., Iakoucheva, L. M. & Obradovic, Z. (2002). Intrinsic disorder and protein function. *Biochemistry*, **41**, 6573–6582.
13. Dunker, A. K. & Obradovic, Z. (2001). The protein trinity–linking function and disorder. *Nature Biotechnol.* **19**, 805–806.
14. Dunker, A. K., Brown, C. J. & Obradovic, Z. (2002). Identification and functions of usefully disordered proteins. *Advan. Protein Chem.* **62**, 25–49.
15. Gunasekaran, K., Tsai, C.-J., Kumar, S., Zanuy, D. & Nussinov, R. (2003). Extended disordered proteins: targeting function with less scaffold. *Trends Biochem. Sci.* **28**, 81–85.
16. Iakoucheva, L. M., Brown, C. J., Lawson, J. D., Obradovic, Z. & Dunker, A. K. (2002). Intrinsic disorder in cell-signaling and cancer-associated proteins. *J. Mol. Biol.* **323**, 573–584.
17. Namba, K. (2001). Roles of partly unfolded conformations in macromolecular self-assembly. *Genes Cells*, **6**, 1–12.
18. Tompa, P. (2002). Intrinsically unstructured proteins. *Trends Biochem. Sci.* **27**, 527–533.
19. Uversky, V. N. (2002). Natively unfolded proteins: a point where biology waits for physics. *Protein Sci.* **11**, 739–756.
20. Uversky, V. N. (2003). Protein folding revisited A polypeptide chain at the folding-misfolding-nonfolding crossroads: Which way to go? *Cell. Mol. Life Sci.* **60**, 1852–1871.
21. Farrell, H. M., Jr, Qi, P. X., Brown, E. M., Cooke, P. H., Tunick, M. H., Wickham, E. D. & Unruh, J. J. (2002). Molten globule structures in milk proteins: implications for potential new structure-function relationships. *J. Dairy Sci.* **85**, 459–471.
22. Schulman, B. A., Redfield, C., Peng, Z.-y., Dobson, C. M. & Kim, P. S. (1995). Different subdomains are most protected from hydrogen exchange in the molten globule and native states of human α-lactalbumin. *J. Mol. Biol.* **253**, 651–657.
23. Bañuelos, S. & Muga, A. (1995). Binding of molten globule-like conformations to lipid bilayers. *J. Biol. Chem.* **270**, 29910–29915.
24. Alexandrescu, A. T., Ng, Y. L. & Dobson, C. M. (1994). Characterization of a trifluoroethanol-induced partially folded state of alpha-lactalbumin. *J. Mol. Biol.* **235**, 587–599.
25. Laureto, P. P. d., Frare, E., Gittardo, R. & Fontana, A. (2002). Molten globule of bovine alpha-lactalbumin at neutral pH induced by heat, trifluoroethanol, and

oleic acid: a comparative analysis by circular dichroism spectroscopy and limited proteolysis. *Proteins: Struct. Funct. Genet.* **49**, 385–397.
26. Permyakov, E. A. & Berliner, L. J. (2000). α-Lactalbumin: structure and function. *FEBS Letters*, **473**, 269–274.
27. Forge, V., Wijesinha, R. T., Balbach, J., Brew, K., Robinson, C. V., Redfield, C. & Dobson, C. M. (1999). Rapid collapse and slow structural reorganisation during the refolding of bovine α-lactalbumin. *J. Mol. Biol.* **288**, 673–688.
28. Lala, A. K. & Kaul, P. (1992). Increased exposure of hydrophobic surface in molten globule state of alpha-lactalbumin-fluorescence and hydrophobic photolabeling studies. *J. Biol. Chem.* **267**, 19914–19918.
29. Bañuelos, S. & Muga, A. (1996). Interaction of native and partially folded conformations of α-lactalbumin with lipid bilayers: characterization of two membrane-bound states. *FEBS Letters*, **386**, 21–58.
30. Agasøster, A. V., Halskau, Ø., Fuglebakk, E., Frøystein, N. Å., Muga, A., Holmsen, H. & Martínez, A. (2003). The interaction of peripheral proteins and membranes studied with alpha-lactalbumin and phospholipid bilayers of various compositions. *J. Biol. Chem.* **278**, 21790–21797.
31. Sinibaldi, F., Howes, B. D., Smulevich, G., Ciaccio, C., Coletta, M. & Santucci, R. (2003). Anion concentration modulates the conformation and stability of the molten globule of cytochrome c. *J. Biol. Inorg. Chem.* **8**, 663–670.
32. Bertini, I., Turano, P., Vasos, P. R., Bondon, A., Chevance, S. & Simonneaux, G. (2004). Cytochrome c and SDS: a molten globule protein with altered axial ligation. *J. Mol. Biol.* **336**, 489–496.
33. Chattopadhyay, K. & Mazumdar, S. (2003). Stabilization of partially folded states of cytochrome c in aqueous surfactant: effects of ionic and hydrophobic interactions. *Biochemistry*, **42**, 14606–14613.
34. Hamada, S. & Takeda, K. (1993). Conformational changes of alpha-lactalbumin and its fragment, Phe31-Ile59, induced by sodium dodecyl sulfate. *J. Protein Chem.* **12**, 477–482.
35. Lindberg, M., Biverstahl, H., Graslund, A. & Maler, L. (2003). Structure and positioning comparison of two variants of penetratin in two different membrane mimicking systems by NMR. *Eur. J. Biochem.* **270**, 3055–3063.
36. Ohman, A., Lycksell, P. O., Jureus, A., Langel, U., Bartfai, T. & Graslund, A. (1998). NMR study of the conformation and localization of porcine galanin in SDS micelles. Comparison with an inactive analog and a galanin receptor antagonist. *Biochemistry*, **37**, 9169–9178.
37. Losonczi, J. A., Olejniczak, E. T., Betz, S. F., Harlan, J. E., Mack, J. & Fesik, S. W. (2000). NMR studies of the anti-apoptotic protein Bcl-xL in micelles. *Biochemistry*, **39**, 11024–11033.
38. Glaser, R. W., Grune, M., Wandelt, C. & Ulrich, A. S. (1999). Structure analysis of a fusogenic peptide sequence from the sea urchin fertilization protein bindin. *Biochemistry*, **38**, 2560–2569.
39. Grace, R. C., Lynn, A. M. & Cowsik, S. M. (2001). Lipid induced conformation of the tachykinin peptide Kassinin. *J. Biomol. Struct. Dynam.* **18**, 611–621 see also pp. 623–625.
40. Cawthern, K. M., Permyakov, E. & Berliner, L. J. (1996). Membrane-bound states of alpha-lactalbumin: implications for the protein stability and conformation. *Protein Sci.* **5**, 1394–1405.
41. Balbach, J., Forge, V., Lau, W. S., Nuland, N. A. J. v., Brew, K. & Dobson, C. M. (1996). Protein folding monitored at individual residues during a two-dimensional NMR experiment. *Science*, **274**, 1161–1163.
42. Halskau, Ø., Frøystein, N. Å., Muga, A. & Martínez, A. (2002). The membrane-bound conformation of α-lactalbumin studied by NMR-monitored ^{1}H exchange. *J. Mol. Biol.* **321**, 99–110.
43. Lala, A. K., Kaul, P. & Ratnam, P. B. (1995). Membrane-protein interaction and the molten globule state: interaction of alpha-lactalbumin with membranes. *J. Protein Chem.* **14**, 601–609.
44. Moosavi-Movahedi, A. A., Chamani, J., Goto, Y. & Hakimelahi, G. H. (2003). Formation of the molten globule-like state of cytochrome *c* induced by *n-alkyl* sulfates at low concentrations. *J. Biochem. (Tokyo)*, **133**, 93–102.
45. Griko, Y. V. (2000). Energetic basis of structural stability in the molten globule state: alpha-lactalbumin. *J. Mol. Biol.* **297**, 1259–1268.
46. Rao, M. V., Atreyi, M. & Rajeswari, M. R. (1981). Fluorescence spectra of lysozyme excited at 305 nm in presence of urea. *Int. J. Pept. Protein Res.* **17**, 205–210.
47. Joseph, M. & Nagaraj, R. (1992). Unfolding of lysozyme by breaking its disulphide bridges results in exposure of hydrophobic sites. *Biochem. Int.* **26**, 973–978.
48. Bohm, G., Muhr, R. & Jaenicke, R. (1992). Quantitative analysis of protein far UV circular dichroism spectra by neural networks. *Protein Eng.* **5**, 191–195.
49. Alexandrescu, A. T., Broadhurst, R. W., Wormald, C., Chyan, C. L., Baum, J. & Dobson, C. M. (1992). 1H-NMR assignments and local environments of aromatic residues in bovine, human and guinea pig variants of alpha-lactalbumin. *Eur. J. Biochem.* **210**, 699–709.
50. Dobson, C. M., Sali, A. & Karplus, M. (1998). Protein folding: a perspective from theory and experiment. *Angew. Chem. Int. Ed.* **37**, 868–893.
51. Wijesinha-Bettoni, R., Dobson, C. M. & Redfield, C. (2001). Comparison of the denaturant-induced unfolding of the bovine and human alpha-lactalbumin molten globules. *J. Mol. Biol.* **312**, 261–273.
52. Ramboarina, S. & Redfield, C. (2003). Structural characterisation of the human alpha-lactalbumin molten globule at high temperature. *J. Mol. Biol.* **330**, 1177–1188.
53. Grobler, J. A., Wang, M., Pike, A. C. & Brew, K. (1994). Study by mutagenesis of the roles of two aromatic clusters of alpha-lactalbumin in aspects of its action in the lactose synthase system. *J. Biol. Chem.* **269**, 5106–5114.
54. Chaudhuri, T. K., Horii, K., Yoda, T., Arai, M., Nagata, S., Terada, T. P. *et al.* (1999). Effect of the extra N-terminal methionine residue on the stability and folding of recombinant alpha-lactalbumin expressed in *Escherichia coli*. *J. Mol. Biol.* **285**, 1179–1194.
55. Delaglio, F., Zhu, G. & Bax, A. (2001). Measurement of homonuclear proton couplings from regular 2D COSY spectra. *J. Magn. Reson.* **149**, 276–281.
56. Nilges, M., Macias, M. J., O'Donoghue, S. I. & Oschkinat, H. (1997). Automated NOESY interpretation with ambiguous distance restraints: the refined NMR solution structure of the pleckstrin homology domain from beta-spectrin. *J. Mol. Biol.* **269**, 408–422.
57. Wishart, D. S., Sykes, B. D. & Richards, F. M. (1992).

The chemical shift index: a fast and simple method for for the assignment of secondary structure through NMR spectroscopy. *Biochemistry*, **31**, 1647–1651.
58. Chrysina, E. D., Brew, K. & Acharya, K. R. (2000). Crystal structures of apo- and holo-bovine alpha-lactalbumin at 2.2-Å resolution reveal an effect of calcium on inter-lobe interactions. *J. Biol. Chem.* **275**, 37021–37029.
59. Pike, A. C., Brew, K. & Acharya, K. R. (1996). Crystal structures of guinea-pig, goat and bovine a-lactalbumin highlight the enhanced conformational flexibility of regions that are significant for its action in lactose synthase. *Structure*, **4**, 691–703.
60. Malinovskii, V. A., Tian, J., Grobler, J. A. & Brew, K. (1996). Functional site in alpha-lactalbumin encompasses a region corresponding to a subsite in lysozyme and parts of two adjacent flexible substructures. *Biochemistry*, **35**, 9710–9715.
61. Greene, L. H., Grobler, J. A., Malinovskii, V. A., Tian, J., Acharya, K. R. & Brew, K. (1999). Stability, activity and flexibility in alpha-lactalbumin. *Protein Eng.* **12**, 581–587.
62. Ramakrishnan, B. & Qasba, P. K. (2001). Crystal structure of lactose synthase reveals a large conformational change in its catalytic component, the beta1,4-galactosyltransferase-I. *J. Mol. Biol.* **310**, 205–218.
63. Svensson, M., Sabharwal, H., Hakansson, A., Mossberg, A. K., Lipniunas, P., Leffler, H. *et al*. (1999). Molecular characterization of alpha-lactalbumin folding variants that induce apoptosis in tumor cells. *J. Biol. Chem.* **274**, 6388–6396.
64. Svensson, M., Hakansson, A., Mossberg, A. K., Linse, S. & Svanborg, C. (2000). Conversion of alpha-lactalbumin to a protein inducing apoptosis. *Proc. Natl Acad. Sci. USA*, **97**, 4221–4226.
65. Svensson, M., Duringer, C., Hallgren, O., Mossberg, A. K., Hakansson, A., Linse, S. & Svanborg, C. (2002). Hamlet–a complex from human milk that induces apoptosis in tumor cells but spares healthy cells. *Advan. Expt. Med. Biol.* **503**, 125–132.
66. Svensson, M., Fast, J., Mossberg, A. K., Duringer, C., Gustafsson, L., Hallgren, O. *et al*. (2003). Alpha-lactalbumin unfolding is not sufficient to cause apoptosis, but is required for the conversion to HAMLET (human alpha-lactalbumin made lethal to tumor cells). *Protein Sci.* **12**, 2794–2804.
67. Casbarra, A., Birolo, L., Infusini, G., Dal Piaz, F., Svensson, M., Pucci, P. *et al*. (2004). Conformational analysis of HAMLET, the folding variant of human alpha-lactalbumin associated with apoptosis. *Protein Sci.* **13**, 1322–1330.
68. Sivaraman, T., Kumar, T. K. & Yu, C. (1996). Destabilisation of native tertiary structural interactions is linked to helix-induction by 2,2,2-trifluoroethanol in proteins. *Int. J. Biol. Macromol.* **19**, 235–239.
69. Deber, C. M. & Li, S. C. (1995). Peptides in membranes: helicity and hydrophobicity. *Biopolymers*, **37**, 295–318.
70. Verza, G. & Bakas, L. (2000). Location of tryptophan residues in free and membrane bound *Escherichia coli* alpha-hemolysin and their role on the lytic membrane properties. *Biochim. Biophys. Acta*, **1464**, 27–34.
71. Matsunaga, Y., Ierovnik, E., Yamada, T. & Turk, V. (2002). Conformational changes preceding amyloid-fibril formation of amyloid-beta and stefin B; parallels in pH dependence. *Curr. Med. Chem.* **9**, 1717–1724.
72. Miura, T., Mitani, S., Takanashi, C. & Mochizuki, N. (2004). Copper selectively triggers beta-sheet assembly of an N-terminally truncated amyloid beta-peptide beginning with Glu3. *J. Inorg. Biochem.* **98**, 10–14.
73. Lindberg, M. & Graslund, A. (2001). The position of the cell penetrating peptide penetratin in SDS micelles determined by NMR. *FEBS Letters*, **497**, 39–44.
74. Bisaglia, M., Tessari, I., Pinato, L., Bellanda, M., Giraudo, S., Fasano, M. *et al*. (2005). A topological model of the interaction between alpha-synuclein and sodium dodecyl sulfate micelles. *Biochemistry*, **44**, 329–339.
75. Bychkova, V. E., Pain, R. H. & Ptitsyn, O. B. (1988). The "molten globule" state is involved in the translocation of proteins across membranes? *FEBS Letters*, **238**, 231–234.
76. Lippens, G., Dhalluin, C. & Wieruszewsky, J. M. (1995). Use of a water flip-back pulse in the hononuclear NOESY experiment. *J. Biomol. NMR*, **5**, 327–331.
77. Zijl, P. C. M. v., Johnson, M. O. N., Mori, S. & Hurd, R. E. (1995). Magic-angle double-quantum-filtered COSY. *J. Magn. Reson.* **113**, 265–270.
78. Krishnamurthy, V. V. (1997). Application of semi-selective excitation sculpting for homonuclear decoupling during evolution in multi-dimensional NMR. *Magn. Reson. Chem.* **35**, 9–12.
79. Hwang, T.-L. & Shaka, A. J. (1994). Water suppression that works. Excitation sculpting using arbitrary waveforms and pulse field gradients. *J. Magn. Reson. ser. A*, **112**, 275–279.
80. Brunger, A. T., Adams, P. D., Clore, G. M., DeLano, W. L., Gros, P., Grosse-Kunstleve, R. W. *et al*. (1998). Crystallography & NMR system: a new software suite for macromolecular structure determination. *Acta Crystallog. sect. D*, **54**, 905–921.
81. Koradi, R., Billeter, M., Engeli, M., Guntert, P. & Wuthrich, K. (1998). Automated peak picking and peak intergration in macromolecular NMR spectra using AUTOPSY. *J. Magn. Reson.* **135**, 288–297.
82. Wishart, D. S., Sykes, B. D. & Richards, F. M. (1991). Realtionship between NMR chemical-shift and protein secondary structure. *J. Mol. Biol.* **222**, 311–333.

Edited by K. Kuwajima

(Received 7 January 2005; received in revised form 4 April 2005; accepted 12 April 2005)